

REPORT

OPEN ACCESS



Liposomal T cell engager and re-director for tumor cell eradication in cancer immunotherapy

Fang Xie^a, Luchen Zhang^a, Sanyuan Shi^a, Anjie Zheng^a, Jiaying Di^a, Shanshan Jin^b, Xuguang Miao^a, Fenglan Wu^a, Xiaolong Chen^b, Yanhong Zhang^b, Xiaohui Wei^a, and Yuhong Xu^{b,c}

^aSchool of Pharmacy, Shanghai Jiao Tong University, Shanghai, Jiangsu, China; ^bR&D department, Hangzhou Highfield Bipharmaceuticals Ltd, Hangzhou, Zhejiang, China; ^cSchool of Pharmacy, Dali University, Dali, Yunnan, China

ABSTRACT

T cells are one of the most important effector cells in cancer immunotherapy. Various T cell-dependent bispecific antibody (TDB) drugs that engage T cells for targeted cancer cell lysis are being developed. Here, we describe supra-molecular T-cell redirecting antibody fragment-anchored liposomes (TRAFsomes) and report their immune modulation and anti-cancer effects. We found that TRAFsomes containing different copies of anti-CD3 fragments displayed different T cell modulation profiles, showing that optimization of surface density is needed to define the therapeutic window for potentiating cancer cell-specific immune reactions while minimizing nonspecific side effects. Moreover, small molecular immunomodulators may also be incorporated by liposomal encapsulation to drive CD8 + T cell biased immune responses. In vivo studies using human peripheral blood mononuclear cell reconstituted mouse models showed that TRAFsomes remained bounded to human T cells and persisted for more than 48 hours after injection. However, only TRAFsomes containing a few anti-CD3 (n = 9) demonstrated significant T cell-mediated anti-cancer activities to reverse tumor growth. Those with more anti-CD3s (n = 70) caused tumor growth and depletion of human T cells at the end of treatments. These data suggested that TRAFsomes can be as potent as traditional TDBs and the liposomal structure offers great potential for immunomodulation and improvement of the therapeutic index.

Abbreviation: Chimeric antigen receptor T cells (CAR-T cells), Cytokine release syndrome (CRS) Cytotoxic T cell (CTL) Effector: target ratios (E:T ratios), Heavy chain (HC) Immune-related adverse events (irAE), Large unilamellar vesicle (LUV), Peripheral blood mononuclear cells (PBMCs), Single-chain variable fragment (scFv), T cell-dependent bispecific antibody (TDB), T cell redirecting antibody fragment-anchored liposomes (TRAFsomes), Methoxy poly-(ethylene glycol) (mPEG)

ARTICLE HISTORY

Received 7 March 2022
Revised 25 Jul 2022
Accepted 16 August 2022

KEYWORDS

T-cell dependent bispecific antibody (TDB); anti-CD3; anti-CD19; liposome; T cell engager

Introduction

Engineering T cell immunity using chimeric antigen receptor T cells (CAR-T cells) or T cell-dependent bispecific antibodies (TDBs) has been successful, especially for blood cancer treatments.¹ These two approaches share the same key feature: the use of an antibody fragment to enable specific tumor cell recognition by polyclonal T cells. CAR-T cells are designed to express single-chain variable fragments (scFvs) on the cell surface, while TDBs bind to T cells *in situ*. The first-in-class TDB product blinatumomab contains two scFvs connected in tandem and has a molecular weight (MW) of ~54.1 kDa.² It is highly potent, with an EC₅₀ at the picomolar range *in vitro*, but *in vivo* it has a very short serum half-life (~1.25 hr in human) and narrow therapeutic window.²

Substantial efforts are being made to improve TDB designs by varying the antibody affinity, avidity, stability and using formats such as diabody and knobs-into-holes.^{1,3-5} Furthermore, recent studies have proposed to add costimulatory molecules, checkpoint blockers, or metabolic and epigenetic modulators to tune T cell reactivities.^{6,7} Small molecular drugs were found to be able to modulate T cell signaling. PI3K and mTOR inhibitors may

affect memory T cells,⁸ while dasatinib has been shown to mitigate cytokine release syndrome (CRS) and immune-related adverse events (irAE).⁹ They were proposed to be used as “switches” in T cell-based immunotherapy.

In order to construct and combine the different immunomodulatory components, we describe here the development and optimization of T cell Redirecting Antibody Fragment-anchored Liposomes (TRAFsomes). Antibody fragments were anchored onto liposomal surfaces for interaction with various cell surface receptors.¹⁰ Such a format enabled multivalent and multispecific interactions and resulted in T cell engagement and cancer cell lysis. Several reports have described similar nano-sized liposomes or nanoparticles coated with anti-CD3, anti-CD40, anti-4-1BB, anti-PD-1, or anti-LAG-3,¹¹⁻¹⁴ but specific details about their immune-modulation effects are lacking, especially in reference to TDBs. We examined TRAFsomes with varying stoichiometries of anti-CD3 and anti-CD19 Fab' and compared their binding and T cell engaging properties. The results were analyzed to understand the unique immune modulation aspects of TRAFsomes as compared to those reported in blinatumomab studies. The

liposome pharmacokinetic properties and various temporal features of T cell subsets activation were analyzed. Furthermore, we showed that TRAFsomes encapsulating certain doses of dasatinib exerted biased modulation of CD8 + T cells before inhibiting all T cell activities at higher doses. An in vivo study demonstrated how the multiplicity of CD3 engagement may affect the resulting T cell activities and immunotherapy outcomes. These understandings are crucial for developing TRAFsomes as a new TDB format for cancer treatment.

Results

TRAFsome preparation and characterization

The TRAFsomes were prepared by decorating pre-formed liposomes with both an anti-CD3 Fab' and an anti-CD19 Fab' (Figure 1a). In brief, Fab' was obtained by selectively reducing bivalent F(ab')₂ to expose the thiol group in the hinge region and reacted with DSPE-PEG-maleimide to generate Fab'-PEG-DSPE. The conjugates were analyzed in gel electrophoresis (Figure 1b and 1c) and confirmed to be about ~3 kDa larger than Fab' (lane 3) or the enzyme-cleaved heavy-chain bands (lane 6). They were then loaded onto pre-formed HSPC/CHOL/DSPE-PEG liposomes based on the post-insertion method.^{10,15} The pre-formed liposome is highly stable and is not fusogenic.¹⁶ The resulting TRAFsomes had a narrow size distribution as measured by dynamic light scattering (Figure 1d). The average amount of Fab' copies per liposome was calculated by dividing the total incorporated antibody mole concentration with the liposome mole concentration (assuming 64 million Dalton MW for a large unilamellar vesicle (LUV)). The distribution of Fab' copies per liposome may vary on each liposome and only the averaged number was calculated. The variations should be similar to those of the liposome diameters and lipid compositions.¹⁷ The individual numbers may vary, but they should always be within a relatively small range surrounding the mean value. Based on these copy numbers, we could also estimate the corresponding surface density of the Fab' on the liposome surface (Figure 1e).

TRAFsome binding to CD3 + T cells, CD19+ tumor cells, and both

Liposomes containing various copies of anti-CD3 Fab', anti-CD19 Fab', or both were evaluated for their binding toward the respective target cells (Figure 2a-d). Only anti-CD3 containing liposomes were able to bind to CD3-expressing Jurkat cells (Figure 2a). The cell-associated liposome fluorescence was higher with liposomes containing more Fab' copies and saturated when there was an average of nine copies of anti-CD3 Fab' per liposome. Similarly, anti-CD19 Fab'-containing liposomes also bind specifically to CD19-expressing Raji cells, but the saturation threshold was much higher (Figure 2b). These antibody-mediated liposome bindings were target selective, with very little cross-reactivity (Figure 2c-d).

When both CD3+ Jurkat cells and CD19+ Raji cells were present in the 1:1 co-culture system, the addition of TRAFsome caused Jurkat cells interaction with Raji cells (Figure 2e-g). DiI-

labeled Raji cells and CFSE-labeled Jurkat cells were analyzed by fluorescence-activated cell sorting (FACS), where double positive signals were detected only after the addition of TRAFsomes (Figure 2e). Interestingly, TRAFsomes containing more anti-CD3 Fab' (n = 140) led to fewer double positive cells than those with fewer anti-CD3 Fab' (n = 35) (figure 2f). Figure 2g shows a representative microscopic image of liposome mediated association effect between Jurkat cells and Raji cells.

T cell activation and cytotoxic T cell activities triggered by TRAFsomes

The mechanism for TRAFsome engaging T cell activation and triggering cytotoxic T cell (CTL) activities is proposed in Figure 3 a. Based on this mechanism, we examined the T cell-dependent cytotoxicity toward cancer cell after the addition of TRAFsomes or control liposomes. Human peripheral blood mononuclear cells (PBMCs) from healthy donors were co-cultured with four different cancer cells, including the CD19-expressing Raji cells, Daudi cells and K562-CD19 cells. The wildtype K562 cells that are CD19 negative were included for comparison. The 70 × 35 TRAFsome-triggered cytotoxicity at different lipid doses is depicted in Figure 3 33-e. Only TRAFsomes containing both anti-CD3 and anti-CD19 triggered significant CTL activities toward CD19+ cells. Liposomes containing only anti-CD3 may cause some target-independent cell lysis, but always at much higher lipid doses. In K562 cells that were CD19 negative, the cytotoxic effects caused by TRAFsomes were low except when the lipid dose was higher than 10ug/ml. The effects of TRAFsome and anti-CD3 Fab' were similar toward K562 cells, both of which were considered as nonspecific T cell activities. The other control liposomes, the anti-CD19 liposomes and PEG liposomes did not cause any CTL activities across all concentrations.

Figure 3f,g shows the effects of 70 × 35 TRAFsome caused by varying the effector: target (E:T) ratios and incubation time. Since PBMCs from healthy donors contained mostly resting T cells, the TRAFsome-triggered activities were prominent, with higher E:T ratios and longer incubation/stimulation time. However, TRAFsome consistently resulted in higher CTL activities with clear dose correlation (Figure 3g). In addition, TRAFsome-triggered cytotoxicity was not dependent on exogenous interleukin (IL)-2 (Figure 3h).

We also examined the TRAFsome activities using PBMCs from different donors against different cancer cell lines (Figure 3i). TRAFsomes were able to engage T cells for target-specific CTL activities at doses as low as 0.5 µg/ml lipid dose, which is about 8.5 pmol/L nanoparticles and 0.595 nmol/L of anti-CD3 Fab' concentration. Furthermore, TRAFsome treatment was shown to cause increased CD107a expression and interferon (IFN)-γ secretion by T cells (Figure 3j,k), compared to liposomes containing only anti-CD3 Fab' at the same lipid dose.

Optimization of TRAFsome activities by varying antibody copy number and drug encapsulation

Since the anti-CD3 Fab' on the TRAFsome surface not only enabled TRAFsome binding to T cells but also affected T cell

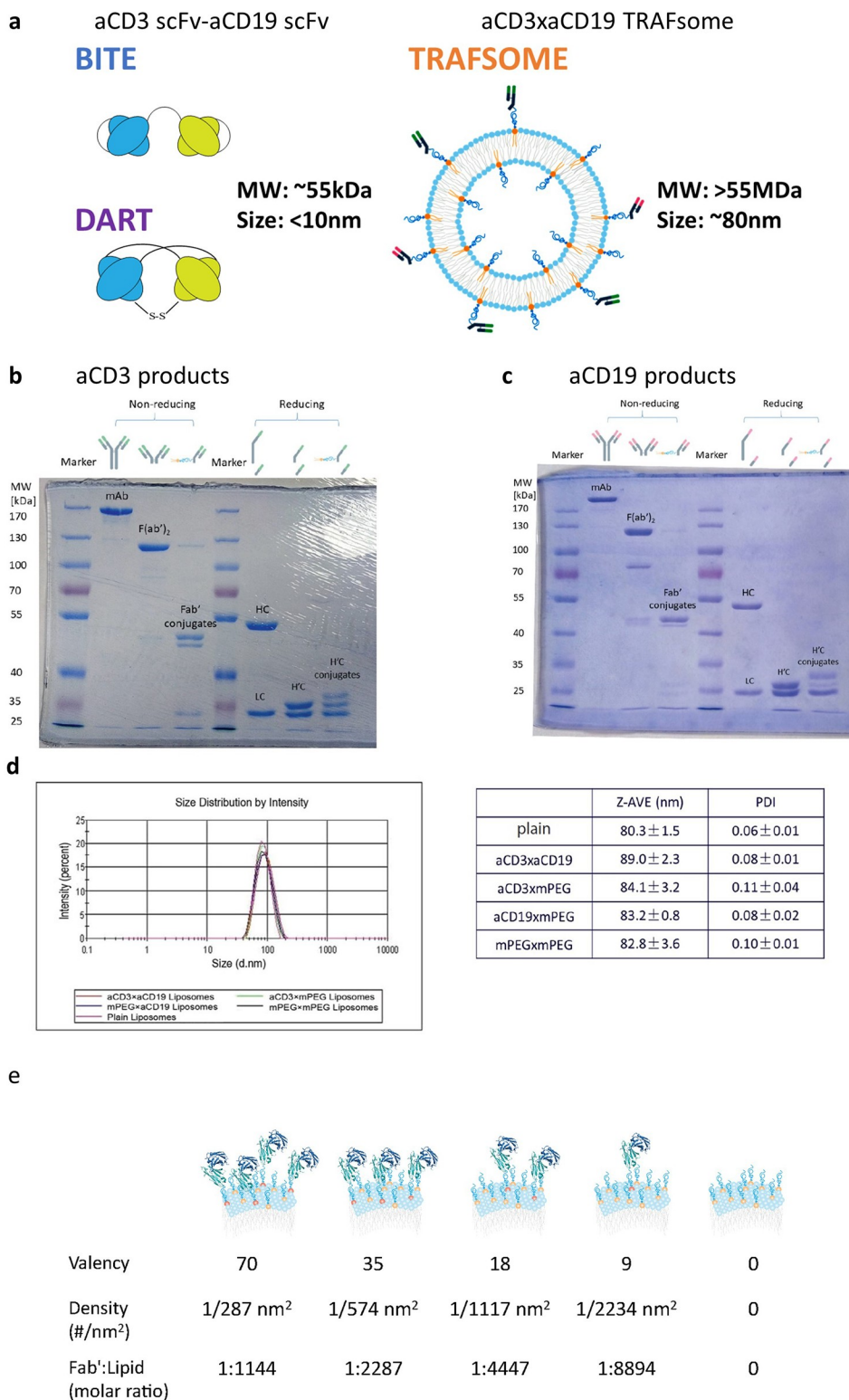


Figure 1. Design and preparation of TRAFsomes. (a) Schematic drawings of different TDB formats, comparing the structures and sizes of BiTE, DART, and TRAFsome. (b-c): anti-CD3 or anti-CD19 Fab' was obtained by enzymatic digestion of IgGs. Fab' was conjugated to DSPE-PEG-mal via maleimide-thiol reaction. These products were analyzed using Polyacrylamide Gel (10%) under non-reducing (lane 1–3) and reducing conditions (lane 4–6). LC: light chain; HC: heavy chain; H'C: enzyme digested heavy chain. (d) Size distributions of TRAFsomes, as measured by dynamic light scattering (DLS). Data shown were means ± SEM (n = 3). (e) Estimated surface densities of antibodies on liposomes containing different copies of Fab'.

activation status, which may cause side effects including cytokine storm, we examined the anti-CD3-mediated T cell activation effects using TRAFsomes containing different copies of anti-CD3 Fab' per TRAFsome (anti-CD3 valency). Both the

T cell activation markers CD69 and CD25 were analyzed. As shown in Figure 4a, the more anti-CD3 Fab' per TRAFsome, the more CD25- and CD69-expressing T cells resulted. Again, liposomes containing only anti-CD3 Fab' caused some degree

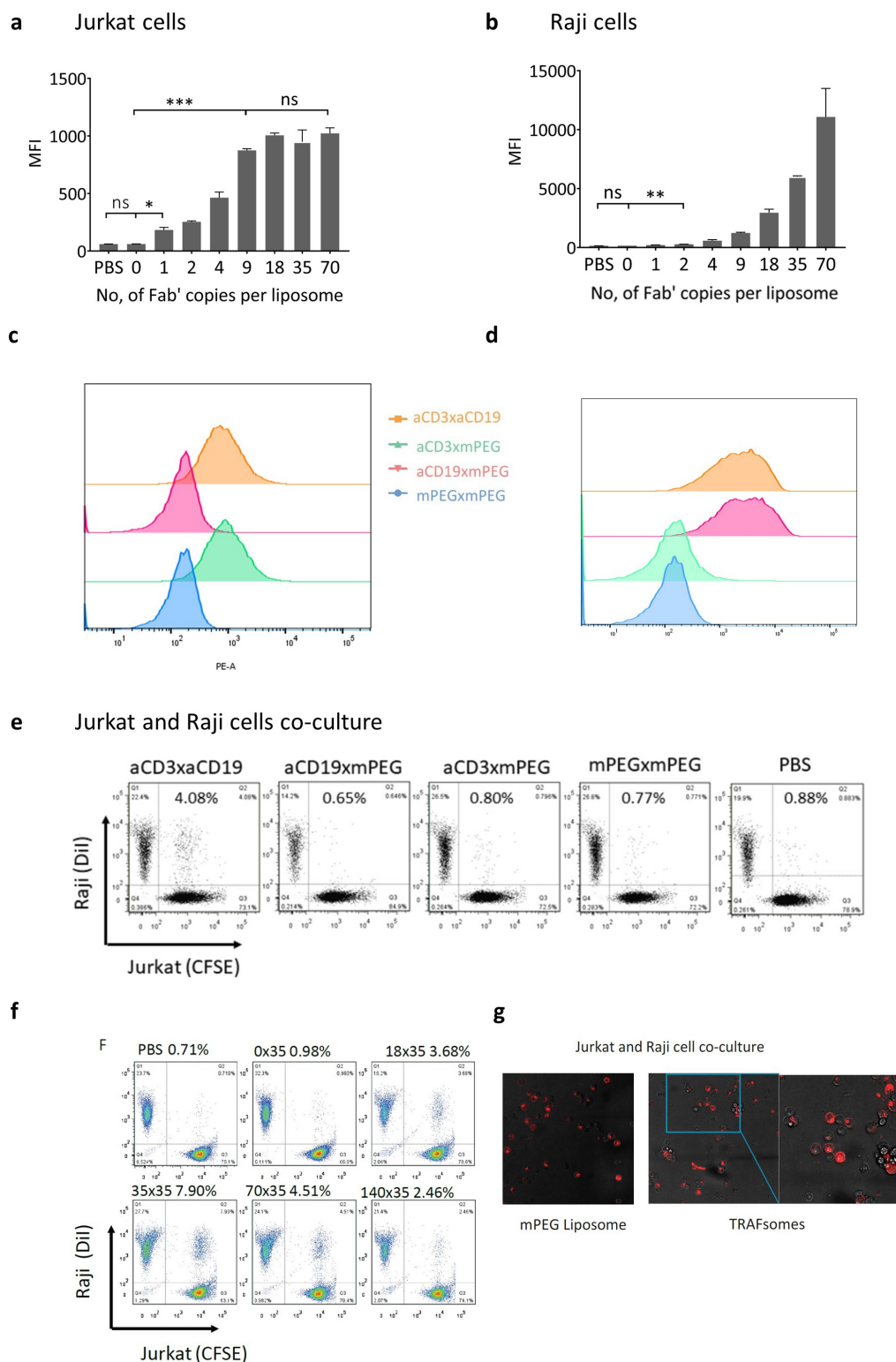


Figure 2. Binding of TRAFsomes to T cells and tumor cells. (a) The effect of anti-CD3 Fab' valency on anti-CD3-liposome binding to hCD3 + T cell leukemia Jurkat cells; (b) The effect of anti-CD19 Fab' valency on anti-CD19-liposome binding to hCD19+ Burkitt lymphoma Raji cells; (c) Binding of Dil-labeled liposomes to Jurkat cells; (d) Binding of Dil-labeled liposomes to Raji cells; (e-f) Cell-cell association between CFSE-labeled Jurkat cells and Dil-labeled Raji cells mediated by TRAFsomes. The FACS dot plots of double positive cells were shown. (g) Representative confocal microscopy images of cross-bridged Raji-Jurkat cell adducts. Jurkat cells (unlabeled) were co-cultured with Dil-labeled Raji cells (red) in presence of mPEGxmPEG Liposomes (left) or TRAFsomes (right). All Liposomes were added at 5 ug/ml. Data shown are mean \pm SEM (n = 3).

of T cell activation when there were more than 18 copies per liposome. Therefore, we conclude that it is very important to limit the number of anti-CD3 Fab' per TRAFsome in order to

minimize nonspecific cell activation. In fact, as shown in Figure 4c, TRAFsomes containing only 9 anti-CD3 could already trigger significant Raji cell lysis, but very little K562

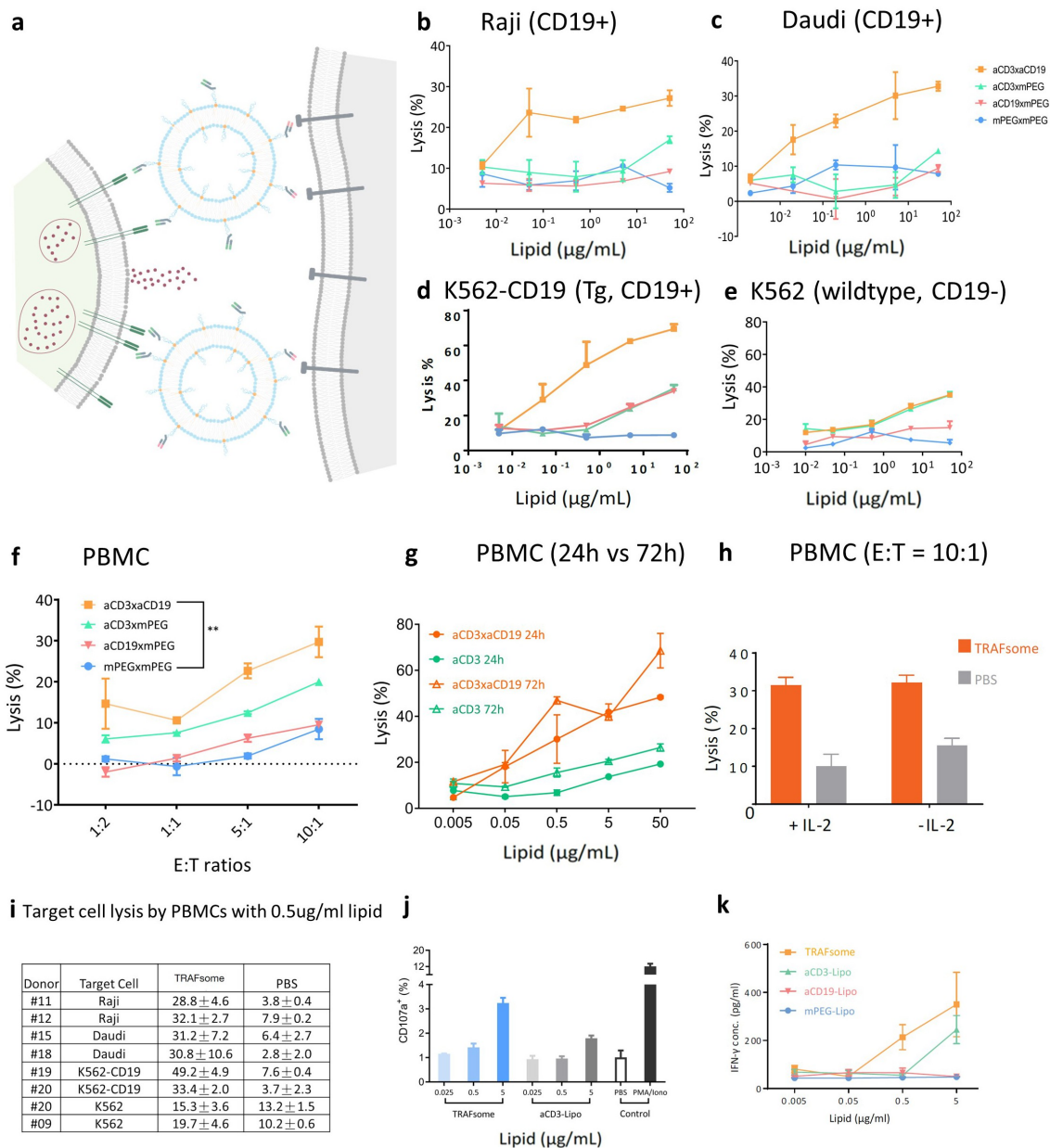


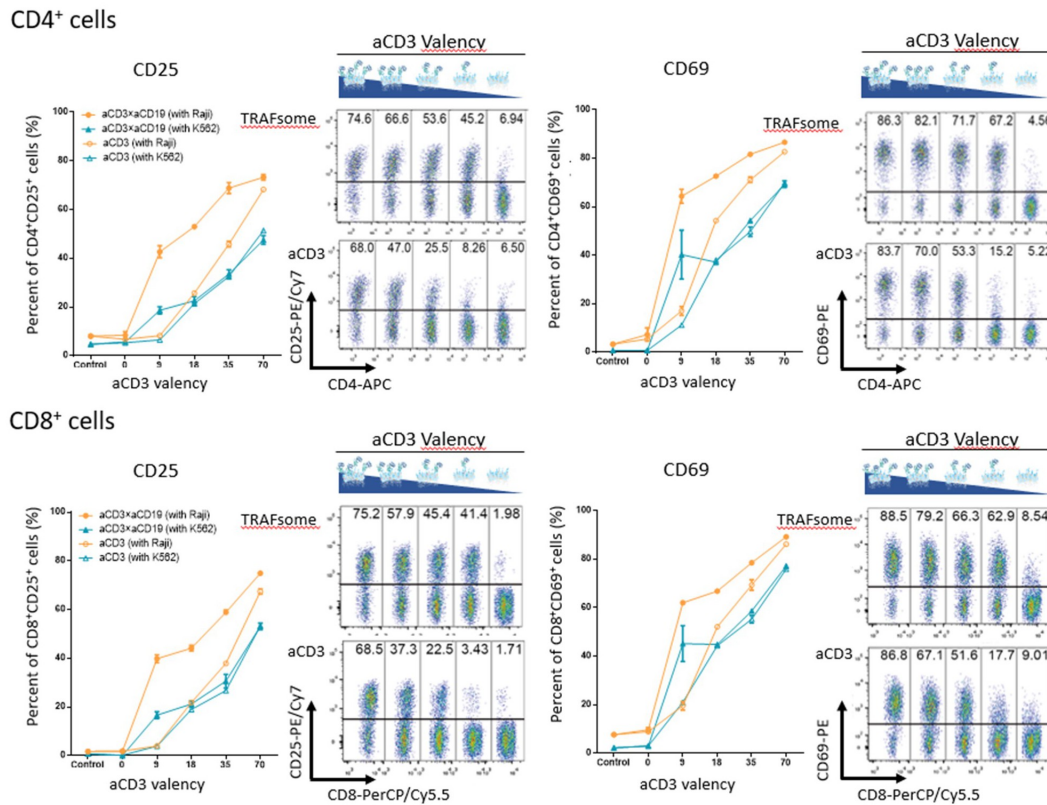
Figure 3. TRAFsomes triggered T cell mediated target cell lysis by PBMCs. (a) Schematic illustration of TRAFsome-mediated CTL responses. (b) Percent of cell lysis by PBMCs triggered by TRAFsomes. (E:T ratio, 10:1; incubation time: 24 h). The target cells were CD19+ Raji cells (b), Daudi cells (c), K562-CD19 cells (d), and CD19 negative K562 cells (e), respectively. (f) Percent of cell lysis triggered by TRAFsomes in the co-culture of PBMCs and Raji cells at different E:T ratios; (g) Percent of CD19+ Raji cell lysis by PBMCs triggered by different doses of TRAFsomes or aCD3-Liposomes. Percent of cell lysis was measured after 24 h or 72 h of incubation. (h) Percent of CD19+ Raji cell lysis by PBMCs triggered by TRAFsome with or without IL2 co-stimulation. (i) Representative target cell lysis by PBMCs from different donors. (Lipid dose at 0.5 ug/ml. E:T ratio at 10:1 and incubation time 24 h). Data shown are mean ± SEM (n = 3). (j) Intracellular CD107a expression by resting PBMC after 5 h of co-culture with Raji cells. PMA and ionomycin stimulation in presence of target cells was used as the positive control. (k) IFN- γ secretion in supernatant after 24 h of co-culture with Raji cells. Results are shown from three independent experiments performed in triplicate wells. Data shown are means ± SEM (n = 3).

cell lysis. On the other hand, anti-CD3 liposomes with higher copies of anti-CD3 Fab' triggered cytotoxicity toward both cells independent of CD19 expression.

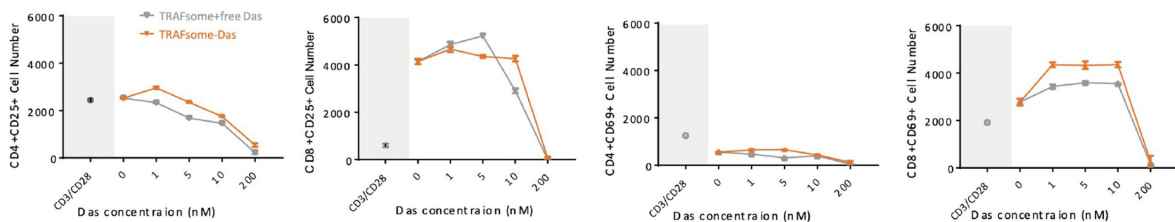
We also explored the encapsulation of dasatinib inside liposomes as another modification to the TRAFsome formulation that might improve CD8+ CTL activities. We first compared the effects of TRAFsome plus the free dasatinib versus TRAFsome-Das on activated CD4+ and CD8+ T cells, while T cells stimulated with both anti-CD3 Fab' and anti-CD28 Fab' were used as the positive control. As expected, dasatinib at the dose of 1–10 nM could significantly improve CD8+ T cell

activation with limited effects on CD4+ T cells (Figure 4b). We then compared the T cell activation profiles of TRAFsomes and TRAFsome-Das in the presence of CD19+ Raji cells and CD19-wildtype K562 cells. As shown in Figure 4d, while the non-specific T cell activation triggered by TRAFsomes at the lipid dose of 5 μ g/ml with K562 were almost as high as those with Raji cell, the addition of TRAFsome-Das notably reduced the non-specific activation. Meanwhile, the CTL activities toward Raji cells were not affected within a TRAFsome-Das dose of 1–10 nM (Figure 4e). We noted that dasatinib at 10 nM and above became inhibitory to T cells, so further optimization of the

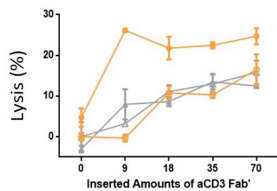
a



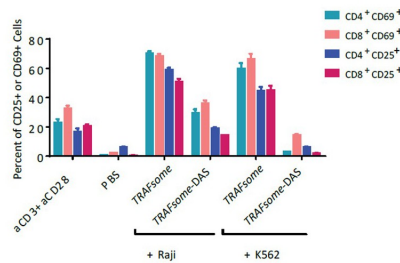
b



c



d



e

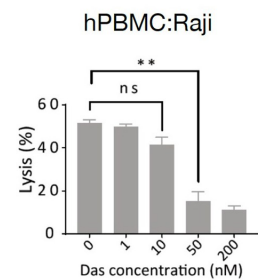


Figure 4. T cell activation by TRAFsomes containing different anti-CD3 copy numbers. (a) T cell activation triggered by TRAFsomes containing different anti-CD3 copy numbers. Lipid dose was 5 μ g/ml. Treatment with plate-bound anti-CD3 plus soluble anti-CD28 or PBS were used as the positive and negative control, respectively. (b) T cell activation after TRAFsomes plus dasatinib or TRAFsomes-Das treatments. Plate-bound anti-CD3 mAb (UCHT1) at equivalent molar concentration (5.6 nmol/L) plus soluble anti-CD28 mAb (2 μ g/ml) were used as the positive control. Data shown are mean \pm SEM (n = 3). (c) T cell lysis of CD19⁺ Raji cells and wildtype K562 cells by TRAFsomes with different anti-CD3 copy numbers; (d) CD25/CD69 expression on CD4⁺ and CD8⁺ T cells triggered by TRAFsomes (70x35) and TRAFsomes-Das (D/L = 0.00075) in the co-culture. Lipid concentration was fixed at 5 μ g/ml. Dasatinib concentration fixed at 5 nM. (e) Raji cell lysis triggered by TRAFsomes-Das at different dasatinib doses. Results were shown from three independent experiments as means \pm SEM (n = 3). *p < .05; **p < .01, by student's t tests.

synergistic combination of TRAFsomes and immunomodulators would be important.

TRAFsomes' activities on $\gamma\delta$ T cells, IL-2 stimulated LAK cells and aCD3/aCD28 bead expanded T cells

The TRAFsomes were found to be able to stimulate other T cell subsets, including $\gamma\delta$ T cells, IL-2-stimulated LAK cells or anti-CD3/anti-CD28 antibodies (aCD3/aCD28) expanded T cells. Compared to freshly isolated PBMCs, these pre-conditioned T cells were considered more reactive. Indeed, TRAFsome treatments led to substantial cytolytic activity by $\gamma\delta$ T cells (44.3% when E:T = 20:1) within 5 hours (hr) of incubation (Figure 5 b 5e-h). Similarly, TRAFsomes trigger much higher CTL activities by IL-2 pre-stimulation LAK cells, compared to mPEG liposomes as well as anti-CD3 liposomes, especially with higher E:T ratios (Figure 5c). Similar activities were seen using aCD3/aCD28 expanded T cells, but the improvement by TRAFsomes over anti-CD3 Fab' only liposomes were small (Figure 5d).

The persistence of TRAFsomes and their interaction with T cells in vivo

Since TRAFsomes contained human anti-CD3 that could only bind to human T cells, this study was done using human PBMC-reconstituted hu-PBL-NOD-SCID mice. The TRAFsomes, as well as liposomes with only anti-CD3 or mPEG, were labeled with Cy5.5 and injected intravenously (iv). Blood samples were drawn at 1 hr, 4 hr, 24 hr and 48 hr after injection (Figure 6a). For the flow cytometry analysis, only those live/hCD45+/hCD3+ cells were gated and their

mean fluorescence intensity (MFI) were plotted. As shown in Figure 6b,c, the human T-cell associated Cy5.5 fluorescence intensities were much higher in the TRAFsome and aCD3-Liposome injected groups, compared to the PEG-Liposome group. The human T-cell associated fluorescence signals were detected for more than 48 hr in both TRAFsomes and aCD3-Liposomes injected mice. Interestingly, at early time points (1 hr and 4 hr), the MFIs were lower in the TRAFsome group compared to the aCD3-Lipo group, likely due to interferences from binding to certain CD19+ cell. The two groups, however, became indistinguishable at the 24 hr and 48 hr time points.

Anti-tumor activities by TRAFsomes with different compositions

The anti-tumor activities of TRAFsomes were tested in a Raji +PBMC co-engraftment model using NOD-*Prkdc^{scid}IL2rg^{tm1}* mice (Figure 7a). Based on the in vitro data, we aimed to compare the dose responses of TRAFsomes with 9 or 70 anti-CD3 valencies (Figure 7b). The CD19+ Raji cells were co-engrafted with PBMC in Matrigel. These Raji+PBMC co-engrafted tumors usually grew slower than Raji (no PBMC) tumors because of the immune system reconstitution. The engrafted tumors were allowed to reach ~200 mm³ before treatments started. The individual tumor growth curves were plotted in Figure 7d and summarized in Figure 7c. Encouragingly, the 9 × 35 TRAFsomes at the low dose of 65 μ g lipid per injection could already effectively shrink the established tumor. Higher doses of the 9 × 35 TRAFsomes resulted in slightly better responses, but, strikingly, we found the treatments of 70 × 35 TRAFsomes at the doses of 133 μ g and 535 μ g lipid (medium and high dose) had no anti-tumor

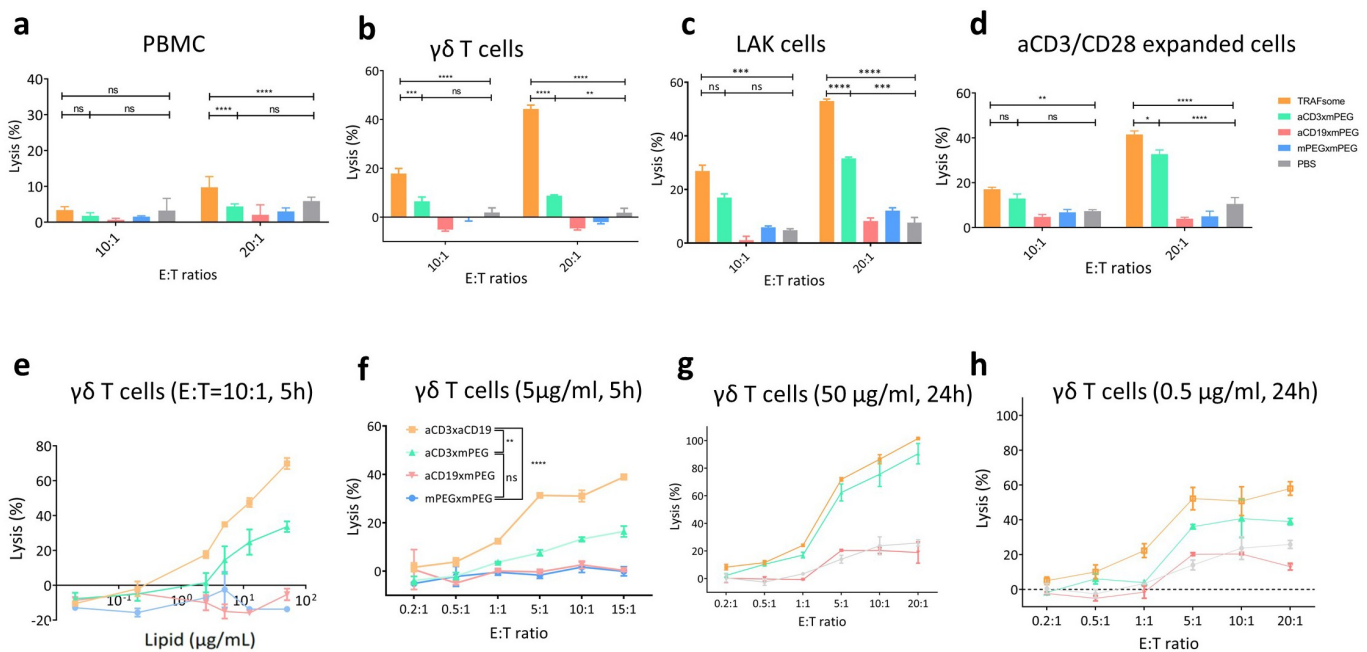


Figure 5. TRAFsomes triggered target cell lysis by various T cell subsets. (a) Raji cell lysis by PBMCs with different effector to target (E:T) ratios after 5 h of co-culture. (b) Raji cell lysis by zoledronic acid primed $\gamma\delta$ T cells with different effector to target (E:T) ratios and after 5 h of co-culture. (c) Raji cell lysis by IL-2 stimulated PBMCs (or lymphokine-activated killer (LAK) cells) after 5 h of co-incubation. (d) Raji cell lysis by aCD3/aCD28 expanded cells after 5 h of co-incubation. (e) Dose-dependent Raji cell lysis by zoledronic acid primed human $\gamma\delta$ T cells. (E:T ratio fixed at 10:1; incubation time at 5 h). (f) Raji cell lysis by zoledronic acid primed human $\gamma\delta$ T cells with different E:T ratios (lipid dose 5 μ g/ml, incubation time 5 h). (g) Raji cell lysis by zoledronic acid primed human $\gamma\delta$ T cells with different E:T ratios (lipid dose 50 μ g/ml and incubation time 24 hr). (h) Raji cell lysis by zoledronic acid primed human $\gamma\delta$ T cells with different E:T ratios (Lipid dose 0.5 μ g/ml and incubation time 24 h). Data shown were means \pm SEM (n = 3). *p < .05; **p < .01; ***p < .001; ****p < .0001 by Student's t test.

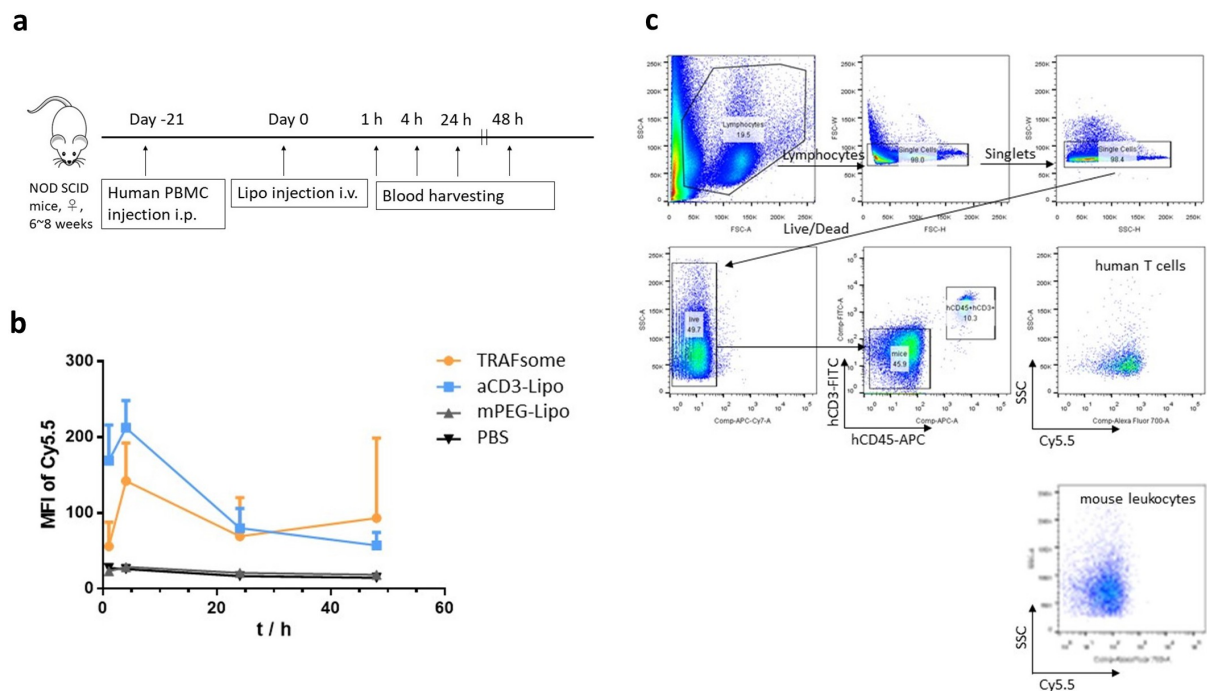


Figure 6. The detection of fluorescence labeled TRAFsomes in PBMCs after iv injection in hu-PBL-SCID mice. Data shown are means \pm SEM ($n = 3$ mice per group). (a) Schematic illustration of the experiment procedure. (b) Mean Fluorescence Intensity (MFI) of Cy5.5 signals of human CD3+ cells collected at different time points. (c) Gating strategies for measuring Cy5.5-labeled TRAFsomes on human CD45+ human CD3+ cells.

effect. In fact, the tumors grew quickly, almost as fast as those in the Raji cell (no PBMC) group. There was, however, an exception: the 70×35 TRAFsomes at the low dose triggered decent anti-tumor activities, similar as those observed in the 9×35 TRAFsome groups.

The mice were sacrificed after the last dose and the remaining hCD3 + T cells in their spleens were analyzed (Figure 7e). We found that there were very few human T cells remaining in 70×35 TRAFsome high- and medium-dose groups. The human T cell numbers in 70×35 TRAFsome low dose and 9×35 TRAFsome medium- and low-dose groups were nearly as high as those in the vehicle control group. The 9×35 TRAFsome high-dose group was a little different, with fewer splenic human T cell remaining, but the tumor growth was much slower.

We also analyzed the blood samples collected on day 26 (24 hr before the last injection) and day 27 (3 hr after the last injection). The percentages of circulating human CD45+ CD3+ in total leukocytes are shown in figure 7f, and the human inflammatory cytokine levels in plasma are shown in Figure 7hg). Notably, the 9×35 TRAFsome high-dose group had decent levels of human T cell numbers and various inflammatory cytokine levels in the plasma.

Discussion

The TRAFsome format described in this study represents a new approach to engineer T cells specificity and activities against target cells. TRAFsomes were made containing anti-CD3 and anti-CD19 antibody fragments, and their respective copy numbers were carefully controlled. Other TDB products usually only contain two binding domains, either scFvs or Fab,

with a 1:1 ratio, but they are usually less than 10 nm in diameter, while TRAFsomes are about 10 times bigger. Since previous studies had assumed that the small size of bispecific T-cell engagers (BiTEs) was a prerequisite for the formation of cytolytic synapses between T cells and the target cells,^{18–20} we have to show that TRAFsomes were also capable of eliciting target cell-specific T cell activation, cytokine release and cytolytic activity (Figure 3–4). We also found that cytolysis was not dependent on IL-2 co-stimulation (Figure 3e), a prominent feature of BiTEs and other small-sized TDBs.²¹ The amount of TRAFsomes required to achieve half maximal cell lysis using PBMC at E:T ratio of 10:1 was about 0.005–0.05 $\mu\text{g}/\text{ml}$ lipids or 0.136–1.36 pmol/L liposomes. The amount of anti-CD3 Fab' was about 10–100 pmol/L. These numbers are similar to the picomolar EC_{50} of Blincyto® (blinatumomab) and other TDBs. We think the lipid bilayer-anchored Fab' format may be more suitable for multivalent interactions with target cell surface proteins because cell membrane proteins in nature can move around on the surface and assemble into clusters. We had previously isolated cell membrane rafts and assembled them on liposomes for multivalent cooperative binding.²² In this case, we may need fewer TRAFsomes than TDBs because the multiple copies of anti-CD3 molecules can bind cooperatively for more efficient T cell engagement.

The use of liposomes or other nanoparticles for assembling cytokines and antibodies for cancer immunotherapy had been reported in several pioneering works.^{11–14,23} In our study, we found that the antibody copy numbers on each liposome play “make or break” roles for the immune stimulation mechanism. For liposomes that contain only 9 Fab', the average surface area per Fab' was about 2234 nm^2 . They may seem to be very far apart, considering the distance between the two Fabs in one

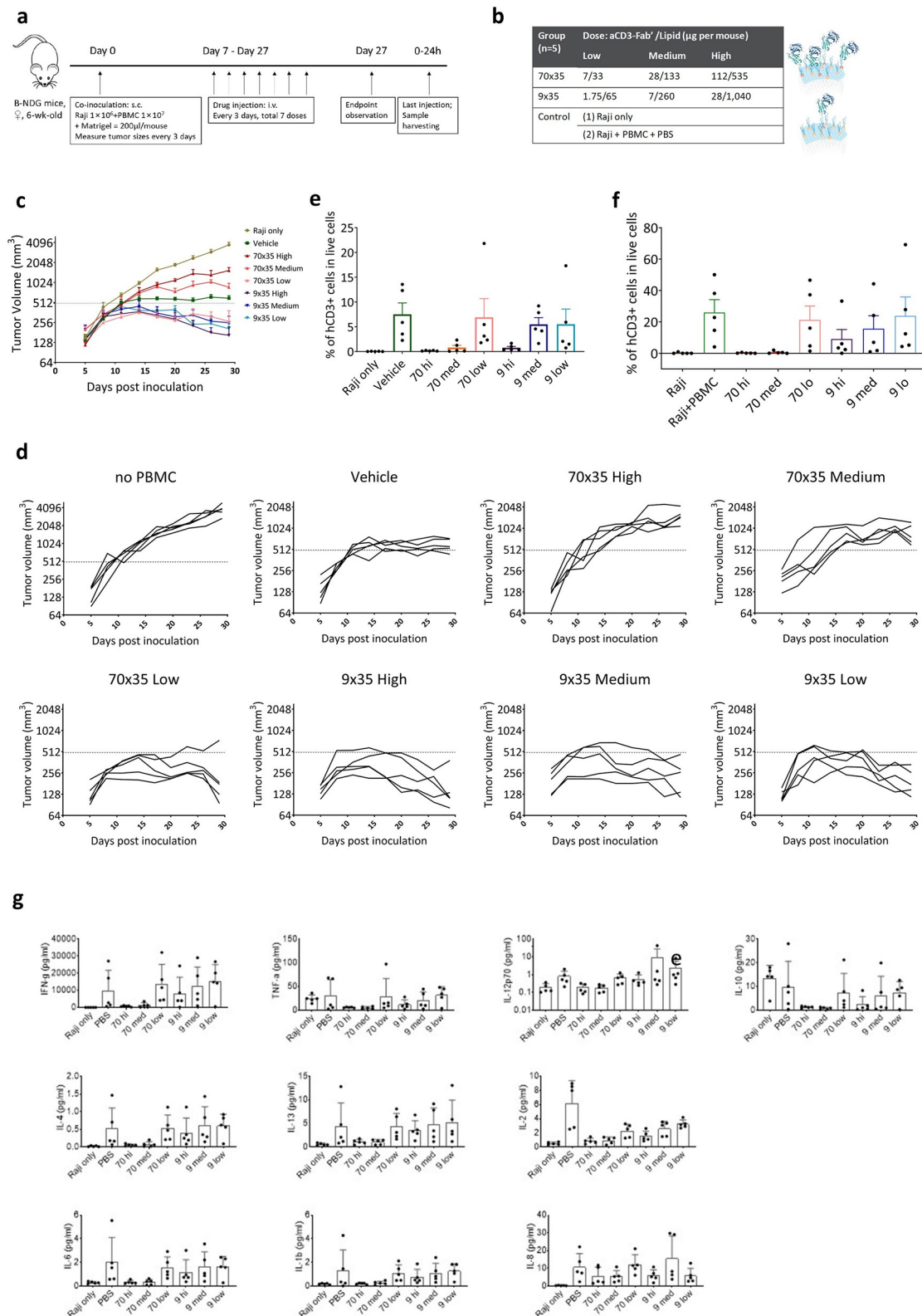


Figure 7. The anti-tumor effect of TRAFsomes with different aCD3xαCD19 compositions. (a-b) experiment setup: NOD-Prkdc^{scid}IL2rg^{tm1} immunodeficient mice were subcutaneously injected with Raji cells (1×10^6) and PBMCs (1×10^7) mixed in Matrigel. Raji cell inoculated mice without human PBMC were included as controls. 9×35 TRAFsomes and 70×35 TRAFsomes were injected every three days starting at 7 days after tumor engraftment. Both TRAFsomes were given in three doses. (c-d) The individual tumor growth curves as well as the average tumor volumes per group (means \pm SEM, $n = 5$) were plotted. Statistics were performed by comparing each group to the vehicle control. (e) Percent of human T cell numbers in spleen at 24 h after the last dose. (f) Percent of circulating human CD45+ CD3+ cells in blood collected at 24 h before the last dosing. (g) Various cytokines levels in serum at 3 h after the last dose. * $p < .05$; ** $p < .01$; *** $p < .001$; **** $p < .0001$, by two-way ANOVA combined with Tukey's multiple comparison test.

IgG, but since they are free to diffuse laterally, their interactions with target cells could still be multivalent, as shown in [Figure 3a](#). In fact, the radius of a TCR density domain was reported to be only about 1–3 nm on naïve T cells and 35–70 nm on activated T cells.¹⁹ Therefore, anti-CD3 are more efficient when present on beads, even though most bead conjugated anti-CD3 are fixed with very limited degree of freedom to cluster. Interestingly, a recent study reported that anti-CD3 conjugated quantum dots with sizes smaller than 50 nm could not activate naïve T cells, but they had better activity toward antigen-experienced T cells, probably because of preexisting TCR clustering.²³ Another study using 2D grid patterned lipid scaffolds showed that at least 2–4 aCD3 agonistic ligands per TCR cluster were required for T cell activation and downstream signaling.²⁰ Increased ligand mobility resulted in faster downstream ZAP70 microclusters formation, heightened intracellular calcium influx and strengthened T cell activation.²⁴ Taken together, lipid bilayers are considered as an ideal scaffold to accommodate protein clustering and cooperative binding, especially in those involving immunological synapses. We found that it took longer for TRAFsomes to activate resting T cells from PBMC than pre-stimulated T cell subsets, probably due to the lack of TCR clustering in resting T cells ([Figure 3](#) and [Figure 5](#)).²⁴ Furthermore, the fact that TRAFsomes were more effective in engaging T cells than anti-CD3 Liposomes with the same copy number indicated that there was also TCR segregation due to cancer cells binding.

Besides efficacy, side effects due to nonspecific T cell activation are another important parameter for evaluating TDBs. It was reported that tandem bispecific-scFvs may cause CD3-crosslinking due to the formation of multimeric scFv aggregates.²⁵ Most TDB doses are limited by toxicities resulting from nonspecific T cell activation. Indeed, we also found that anti-CD3 liposome at 5 µg/ml lipid dose and higher caused target-independent T cell activation. At lipid dose between 0.005 and 5 µg/ml, TRAFsomes were more effective than anti-CD3 liposome, implying a therapeutic window of about 3 orders of magnitude. For pre-stimulated T cell subsets, TRAFsome can activate $\gamma\delta$ T cell effector functions with very fast onset time in both the cognate Daudi cells and the resistant Raji cells.

Furthermore, we also explored the possible advantages of incorporating small molecular immunomodulators inside TRAFsomes for synergistic effects. Dasatinib is a broad kinase inhibitor targeting various Src family kinases but was also found to be involved in T cell effector functions.^{26,27} It was immunosuppressive at high doses, but at moderate doses it can curb Treg cells and rapidly enable large granular lymphocyte mobilization.^{28–30} Several studies have explored the use of dasatinib in combination with anti-OX40 or vaccination for expansions of CD8 + T cell repertoires as opposed to Treg cells.²⁹ In this study, we examined the effects of dasatinib added separately or encapsulated inside TRAFsomes in the hPBMC and Raji cell co-culture system. The CD69 expression on CD8 T cells increased at around 72 hr after the addition of TRAFsome-DAS, a substantial delay compared to the 24 hr time frame in the TRAFsome-only group. There were fewer CD25+ or CD69 + T cells after the treatment with TRAFsome-DAS compared to TRAFsome only, but the reduction was from

~60% to ~40% in the co-culture with Raji cells, and from ~60% to less than 20% in the co-culture with K562 cells ([Figure 4d](#)). The effect was not large, and it was only so at relatively low dasatinib concentrations (i.e., 1–10 nM). Therefore, for in vivo use of TRAFsome-DAS, both the dose ranges of anti-CD3 and dasatinib need to be coordinated and optimized.

Based on these in vitro studies, we then tested the TRAFsome pharmacokinetic and pharmacodynamic behaviors in vivo. We showed that both TRAFsomes and anti-CD3 Liposomes could bind to human T cells within an hour after iv injection and remain bounded for more than 48 hr. Interestingly, the MFI was lower in the TRAFsome group than that of the anti-CD3 liposome group at the early time points, probably because TRAFsomes may also bind to hCD19 + B cells in the peripheral tissues in huPBL-NOD-SCID mice. The human T cell bound fluorescence signals persisted for more than 48 hr in circulation, which could be highly advantageous considering the very short half-life of blinatumomab.

Last but not least, our in vivo pharmacodynamic data revealed the critical role of anti-CD3 copy numbers in the “make or break” of the anti-tumor effects. While TRAFsomes with nine anti-CD3 copies per liposome were highly effective in reversing tumor growth, those containing 70 anti-CD3s Fab’ caused T cell depletion or tolerance. Multi-valent CD3 ligation without IL-2 co-stimulation has been shown to cause T cell anergy, which could lead to failures in T cell-based immunotherapy.^{31,32} Complexed T cell engagers that contain more than one copies of anti-CD3 may be especially of concern.^{1,33} In this regard, nanoparticles and liposomes usually had too many anti-CD3s.^{13,14} We demonstrated that it is possible to alleviate the problem by reducing the anti-CD3 valency, and/or by incorporating immunomodulator inside the liposomes. The engagement of a wider repertoire of T cells including $\gamma\delta$ T cells should also be beneficial, since there may be preexisting tumor evasion mechanisms that compromise tumor antigen-specific T cells.³⁴

Materials and methods

Materials

Lipids used were purchased from Avanti Polar Lipids (Alabaster, AL, USA) unless otherwise noted. 1,2-Distearoyl-sn-glycero-3-phosphoethanolamine-N-[maleimide(polyethylene glycol)-2000 (maleimide-PEG-DSPE), 1,2-Distearoyl-sn-glycero-3-phosphoethanolamine-N-(polyethylene glycol)-2000 (DSPE-PEG2000), cholesterol and hydrogenated Soy l- α -phosphatidylcholine (HSPC) were stored as dry powder at –20°C and dissolved in ethanol immediately before use. Fluorescence labeled lipid, DSPE-PEG2000-Cy5.5, was provided by Xi’an Ruixi Biotech (Xi’an, China). Human anti-CD3 (clone UCHT1) and anti-CD19 (clone 4G7) were from BioXCell (West Lebanon, NH, USA). 2-Mercaptoethanol hydrochloride (2-MEA), Fixable Viability Dye eFluor™ 780, and Carboxyfluorescein diacetate succinimidyl ester (CFSE) were from Thermo Scientific (Rockford, IL, USA). 300 kDa MWCO dialysis device and 50 kDa MWCO dialysis bags were from Spectrum Labs (Rancho Dominguez, CA, USA). Amicon

Ultra-0.5 and Ultra-15 100 kDa MWCO Centrifugal Filter Units were from Millipore (Billerica, MA, USA). 1,1'-Diiodo-3,3',3',3'-Tetramethylindodicarbocyanine perchlorate (DiI), PKH26 Red Fluorescent Cell Linker Kit and Trypan Blue Solution (0.2%) were obtained from Sigma-Aldrich (St. Louis, MO, USA). Recombinant human interleukin-2 (IL-2) was from PeproTech (Rocky Hill, NJ, USA). Ficoll-Paque Plus was from GE Health Care (Waukesha, WI, USA). MojoSort Human CD3+ Cell Isolation Kit, 4',6-Diamidino-2-Phenylindole, Dilactate (DAPI), and 10× red blood cell (RBC) lysis buffer were from BioLegend (San Diego, CA, USA). Flow cytometry staining buffer, fix/perm buffer were from BD Biosciences (San Jose, CA, USA). CytoTox96® Non-Radioactive Cytotoxicity Assay kits were from Promega (Madison, WI, USA). Propidium Iodide (PI) was from Yeasen Biotech (Shanghai, China). Dasatinib (BMS-354825) was purchased from ApexBio (Houston, TX, USA). Zoledronic acid was purchased from Selleck Chemicals (Houston, TX, USA).

F(ab')₂ preparation and bioconjugation

Anti-CD3 and anti-CD19 F(ab')₂ were prepared from UCHT1 and 4G7 using the Mouse IgG1 Fab and F(ab')₂ Preparation Kits from Thermo Scientific (Rockford, IL, USA). The entire process was carried out under N₂ protection using degassed buffers. Fab' was obtained by reducing the purified F(ab')₂ with 5 mM 2-MEA at 37°C for 90 min. The excess 2-MEA was subsequently removed using a 7kD Zeba desalting column. The reduced Fab' was added to DSPE-PEG2000-maleimide solution with 30 mM HEPES (pH 7.0) at 1:1 molar ratio. The reaction was carried out at 10°C for 20 hr in a Thermomixer Shaker (Eppendorf), and stopped by adding 1 mM cysteine and incubated at 4°C for 1 hr.

TRAFsome preparation

LUVs with 80–90 nm mean diameters were prepared as previously described. Anti-CD3 Fab' and anti-CD19 Fab' conjugated lipids were incorporated using the post-insertion method.¹⁷ Anti-CD3 X anti-CD19 TRAFsomes containing both antibodies, anti-CD3xmPEG and anti-CD19xmPEG containing one type of antibodies, as well as PEG-liposomes containing no antibodies were all prepared using the same procedure. They were prepared using the same amount of mPEG-DSPE to substitute the antibody-DSPE. The resulted antibody-decorated liposomes were purified by dialysis in phosphate-buffered saline (PBS) using a 300KD MWCO membrane followed by 5 times washing and re-concentration. The size distribution and polydispersity index (PDI) were determined by dynamic light scattering (DLS, ZetaSizer 3000HSA, Malvern Instruments, UK). The average copy number per liposome was estimated based on the total antibody concentration vs lipid concentration as described previously.³⁵ Briefly, since the liposomes were all about 80 nm in diameter and contain a single bilayer, the lipid mass per liposome was estimated to be 64 million Dalton. The molar ratio of

antibody to liposome was reported as the antibody valency per liposome.

In vitro binding and cell uptake studies

For the cell-binding study, cells were planted in a 24-well plate at 2.5×10^5 cells per well. Fluorescence dye DiI-labeled liposomes were then added (1 μg per well) and incubated for 2 hr at 37°C. After incubation, cells were washed twice with ice-cold PBS, resuspended in 400 μL FACS staining buffer, and analyzed by flow cytometry.

For the cell association study, 1.25×10^5 of CFSE-labeled Jurkat cells were co-cultured with DiI-labeled Raji cells at 1:1 ratio in 500 μl phenol red-free RPMI medium supplemented with 5% fetal bovine serum (FBS) in a 48-well plate. The cell density per well was kept at 5×10^5 per ml to minimize nonspecific cell aggregation. TRAFsome or control liposomes were added and incubated at 37°C for 30 min. The resulted numbers of CFSE and DiI double positive cells were quantified using flow cytometry.

T cell activation and cytotoxicity assays

Primary PBMCs were isolated from healthy human donors using Ficoll-Paque according to the manufacturer's protocol. T cells were isolated using MojoSort human CD3+ isolation kit according to the manufacturer's protocol. The T cell culture medium was prepared by supplementing RPMI culture medium with 10% FBS, HEPES (25 mM), sodium pyruvate (1x), 2-Mercaptoethanol (55μM), non-essential amino acids (NEAA, 1x) (all from GIBCO, Thermo Fisher). γδ T cells were expanded by incubating PBMCs (1 million per ml) in T cell culture medium in the presence of 2 μM zoledronic acid and 200IU/ml IL-2 for 24 hr. The cells were washed and resuspended in a freshly prepared medium containing 200IU/ml IL-2 every three days. The expanded γδ T cells were ready for use on day 12. IL-2-stimulated LAK cells were expanded by incubating PBMCs (1 million per ml) in T cell culture medium containing 1,000 IU/ml IL-2 and were ready for use on day 5. Anti-CD3/anti-CD28 antibodies (aCD3/aCD28) expanded T cells were prepared by incubating PBMCs (1 million per ml) with plate bound anti-CD3 antibody (1μg/ml) plus soluble anti-CD28 antibody (2μg/ml) for 3 days. An equal volume of freshly prepared T cell culture medium (200IU/ml IL-2) was added to each well before the cells were transferred to a new plate and incubated for two days before use. Isolated primary PBMCs or T cells were seeded into 96-well plate at a density of 2×10^5 /well in the presence of target cells at the E:T ratio of 10:1. U-bottom 96-well plates and phenol-free RPMI complete culture medium with 5% FBS (GIBCO) and 50 IU/mL recombinant human IL-2 were used. TRAFsomes or control liposomes were added to each well and incubated at 37°C for 5 hr, 24 hr or 72 hr. After the incubation, T cell mediated cytotoxicity was quantified by measuring lactate dehydrogenase release using the CytoTox96® Non-Radioactive Cytotoxicity Assay kits, and reported as

% Cytotoxicity = (Experimental – Effector Spontaneous – Target Spontaneous)/(Target Maximum – Target Spontaneous) × 100%.

IFN- γ release in the cell culture supernatant after 24 hr of TRAFsome treatments was measured using the human IFN- γ ELISA kit (eBioscience). For the CD107a degranulation assay, 3×10^5 resting PBMCs and 1×10^5 target Raji cells (E:T = 3:1) were co-planted into the wells in a 24-well plate. Then, 4 μ l of PerCP conjugated anti-CD107a (LAMP-1) antibody (H4A3, BioLegend, USA) was quickly added, followed by TRAFsomes or control liposomes. 0.8 μ l of PMA/Ionomycin (500x, eBioscience, Thermo Fisher) treated wells were used as the positive control. After 4 hr of incubation, the transport inhibitor monensin (eBioscience, Thermo Fisher) at 5 μ M was added and incubated for 1 more hour. The cells were collected for flow cytometry analysis.

For the flow cytometry analysis of cell activation, cells were washed and resuspended in staining buffer (BioLegend) after treatment. The cells were then labeled with anti-human CD4 antibody (APC), anti-human CD8 antibody (PerCP-Cy5.5), anti-human CD25 antibody (PE-Cy7) and anti-human CD69 (PE) (all from BioLegend). The cells were washed and resuspended in a staining buffer and stained with 15 μ M PI for 15 minutes on ice just before flow analysis. For the flow cytometry analysis of cytotoxicity, cells were pre-labeled with Cell Tracker PKH26. After the treatment, they were washed and resuspended in staining buffer (BioLegend) and stained with 15 μ M PI for 15 minutes on ice just before flow analysis for apoptosis assay. The flow cytometry analyzed cytotoxicity was reported as % Cytotoxicity = [(apoptotic cell events/total cell events)] \times 100%.

TRAFsome pharmacokinetics study

Human peripheral blood lymphocytes-reconstituted NOD/SCID (Hu-PBL-NOD/SCID) mice were used for the pharmacokinetics study. Briefly, 2×10^7 PBMCs were injected intraperitoneally into each NOD/SCID mouse, and the recipient mouse blood was analyzed by FACS about 4 weeks after the engraftment. Mice that had detectable human CD45+ cells in circulation were considered a successful engraftment and used for the subsequent study. For the pharmacokinetics study, each mouse received an iv injection of 100 μ g of Cy5.5 labeled TRAFsomes (70x35), aCD3-Lipo (70x0), PEG-liposomes or PBS. At the indicated time intervals (i.e., 1 hr, 4 hr, 24 hr and 48 hr), approximately 75 μ L blood was collected in EDTA-K2 pre-treated collection tube. The whole blood samples were treated with RBC lysis buffer, washed, and stained with anti-hCD45 and anti-hCD3 antibodies. The Cy5.5 fluorescence signals on live human CD45+ and CD3+ cells were quantified using the AF700-channel in the flow cytometry.

In vivo anti-tumor efficacy

NOD-*Prkdc^{scid}IL2rg^{tm1}* mice were subcutaneously injected with either 1×10^6 human Burkitt lymphoma Raji cells, or a mixture of 1×10^6 Raji cells and 1×10^7 freshly isolated human PBMCs, supplemented with Matrigel (1:1, v/v) based an established protocol.³⁶ One week after tumor inoculation, mice were randomly divided into groups of five and received iv injections of 200 μ l of TRAFsomes or PBS every 3 days for a total of eight doses. The tumor volumes were measured every 3 days since day 4 after

tumor engraftment. 100 μ l of peripheral blood were drawn into EDTA-K2 pre-treated collection tubes 24 hr before the last dose and 3 hr after the last dose. The mice were sacrificed at 24 hr after the last dose, and spleen and tumor tissues were collected.

The presence of human cytokines in NOD-*Prkdc^{scid}IL2rg^{tm1}* mouse plasma was measured using MSD Proinflammatory Panel 1 (Meso Scale Diagnostics, LLC). The collected mouse whole blood samples were centrifuged at 1,000 g for 10 min and the plasma samples were stored at -80°C before the MSD assay.

Statistical analysis

Statistical analysis was done using GraphPad Prism 7.0 software, and two-tailed unpaired t-tests were conducted. The mean tumor volumes were analyzed with two-way ANOVA with Tukey's multiple comparison. The p values $< .05$ were considered to be significant.

Disclosure statement

Yuhong Xu, ShanShan Jin, Xiaolong Chen, and Yanhong Zhang are employed by Hangzhou Highfield Biopharm and hold company stocks. All other authors declare no conflict of interest.

Data sharing statement

For original data, please contact yhxu@dali.edu.cn

Compliance with ethical standards

Contributions

Fang Xie contributed to the designed, implemented the study and wrote the manuscript; Luchen Zhang, Sanyuan Shi, Anjie Zheng, Jiaying Di, Fenglan Wu and ShanShan Jin participated in some studies, Xuguang Miao, Fenglan Wu, Xiaolong Chen, Yanhong Zhang, and Xiaohui Wei provided critical experiment materials and helped with the data interpretations, Yuhong Xu designed the study, analyzed the data and wrote the manuscript.

Ethical approval

The animal study protocol was approved by the Experimental Animal Management Committee and Experimental Animal Ethics Committee of Shanghai Jiao Tong University following the recommendations in the Guide for the Care and Use of Laboratory Animals (Eighth Edition) and relevant Chinese laws and regulations. All procedures performed in studies involving human participants were in accordance with the ethical standards of the institutional and/or national research committee and with the 1964 Helsinki declaration and its later amendments or comparable ethical standards.

Funding

This study was funded by the National Natural Science Foundation of China (No. 81690262) and Hangzhou Highfield Biopharmaceutical Corp.

ORCID

Yuhong Xu  <http://orcid.org/0000-0001-5302-6392>

References

- Zhukovsky EA, Morse RJ, Maus MV. Bispecific antibodies and CARs: generalized immunotherapeutics harnessing T cell redirection. *Curr Opin Immunol.* 2016;40:24–35. PMID: 26963133. doi:10.1016/j.coi.2016.02.006.
- Klinger M, Brandl C, Zugmaier G, Hijazi Y, Bargou RC, Topp MS, Gökbüget N, Neumann S, Goebeler M, Viardot A, et al. Immunopharmacologic response of patients with B-lineage acute lymphoblastic leukemia to continuous infusion of T cell-engaging CD19/CD3-bispecific BiTE antibody blinatumomab. *Blood.* 2012;119(26):6226–33. PMID: 22592608. doi:10.1182/blood-2012-01-400515.
- Brinkmann U, Kontermann RE. The making of bispecific antibodies. *MAbs.* 2017;9(2):182–212. doi:10.1080/19420862.2016.1268307.
- Slaga D, Ellerman D, Lombana TN, Vij R, Li J, Hristopoulos M, Clark R, Johnston J, Shelton A, Mai E, et al. Avidity-based binding to HER2 results in selective killing of HER2-overexpressing cells by anti-HER2/CD3. *Sci Transl Med.* 2018;10(463). PMID: 30333240. doi:10.1126/scitranslmed.aat5775.
- Klupsch K, Baeriswyl V, Scholz R, Dannenberg J, Santimaria R, Senn D, Kage E, Zumsteg A, Attinger-Toller I, Bey U, et al. COVA4231, a potent CD3/CD33 bispecific FynomAb with IgG-like pharmacokinetics for the treatment of acute myeloid leukemia. *Leukemia.* 2018;33(3):805–08. PMID: 30206306. doi:10.1038/s41375-018-0249-z.
- Correnti C, Laszlo G, de van der Schueren W, Godwin C, Bandaranayake A, Busch M, Gudgeon C, Bates O, Olson J, Mehlin C, et al. Simultaneous multiple interaction T-cell engaging (SMITE) bispecific antibodies overcome bispecific T-cell engager (BiTE) resistance via CD28 co-stimulation. *Leukemia.* 2018;32(5):1239–43. PMID: 29588544. doi:10.1038/s41375-018-0014-3.
- Laszlo G, Gudgeon C, Harrington K, Dell’Ariaga J, Newhall K, Means G, Sinclair A, Kischel R, Frankel S, Walter R. Cellular determinants for preclinical activity of a novel CD33/CD3 bispecific T-cell engager (BiTE) antibody, AMG against human AML. *Blood.* 2014;123(4):554–61. doi:10.1182/blood-2013-09-527044.
- Zheng W, O’Hear C, Alli R, Basham J, Abdelsamed H, Palmer L, Jones L, Youngblood B, Geiger T. PI3K orchestration of the in vivo persistence of chimeric antigen receptor-modified T cells. *Leukemia.* 2018;32(5):1157–67. doi:10.1038/s41375-017-0008-6.
- Mestermann K, Giavridis T, Weber J, Rydzek J, Frenz S, Nerretter T, Mades A, Sadelain M, Einsele H, Hudecek M. The tyrosine kinase inhibitor dasatinib acts as a pharmacologic on/off switch for CAR T cells. *Sci Transl Med.* 2019;11(499):eaau5907. doi:10.1126/scitranslmed.aau5907.
- Manjappa A, Chaudhari K, Venkataraju M, Dantuluri P, Nanda B, Sidda C, Sawant K, Murthy R. Antibody derivatization and conjugation strategies: application in preparation of stealth immunoliposome to target chemotherapeutics to tumor. *J Control Release.* 2011;150(1):2–22. doi:10.1016/j.jconrel.2010.11.002.
- Zhang Y, Li N, Suh H, Irvine D. Nanoparticle anchoring targets immune agonists to tumors enabling anti-cancer immunity without systemic toxicity. *Nat Commun.* 2018;9(1):6. doi:10.1038/s41467-017-02251-3.
- Mi Y, Smith C, Yang F, Qi Y, Roche K, Serody J, Vincent B, Wang A. A dual immunotherapy nanoparticle improves T-cell activation and cancer immunotherapy. *Adv Mater.* 2018;30(25):e1706098. doi:10.1002/adma.201706098.
- Vaidya T, Straubinger R, Ait-Oudhia S. Development and evaluation of tri-functional immunoliposomes for the treatment of HER2 positive breast cancer. *Pharm Res.* 2018;35(5):95. doi:10.1007/s11095-018-2365-x.
- Alhallak K, Sun J, Wasden K, Guenther N, O’Neal J, Muz B, King J, Kohnen D, Vij R, Achilefu S, et al. Nanoparticle T-cell engagers as a modular platform for cancer immunotherapy. *Leukemia.* 2021;35(8):2346–57. PMID: 33479469. doi:10.1038/s41375-021-01127-2.
- Iden D, Allen T. In vitro and in vivo comparison of immunoliposomes made by conventional coupling techniques with those made by a new post-insertion approach. *BBA-Biomembranes.* 2001;1513(2):207–16. doi:10.1016/s0005-2736(01)00357-1.
- Müller M, Zschörnig O, Ohki S, Arnold K. Fusion, leakage and surface hydrophobicity of vesicles containing phosphoinositides: influence of steric and electrostatic effects. *J Membr Biol.* 2003;192(1):33–43. doi:10.1007/s00232-002-1062-0.
- Cliff L, Chadda R, Robertson J. Occupancy distributions of membrane proteins in heterogeneous liposome populations. *Biochim Biophys Acta Biomembr.* 2020;1862(1):183033. doi:10.1016/j.bbame.2019.183033.
- Li J, Stagg N, Johnston J, Harris M, Menzies S, DiCara D, Clark V, Hristopoulos M, Cook R, Slaga D, et al. Membrane-proximal epitope facilitates efficient T cell synapse formation by Anti-FcRH5/CD3 and is a requirement for myeloma cell killing. *Cancer Cell.* 2017;31(3):383–95. PMID: 28262555. doi:10.1016/j.ccell.2017.02.001.
- Lillemeier B, Mörtelmaier M, Forstner M, Huppa J, Groves J, Davis M. TCR and Lat are expressed on separate protein islands on T cell membranes and concatenate during activation. *Nat Immunol.* 2009;11(1):90–96. doi:10.1038/ni.1832.
- Manz B, Jackson B, Petit R, Dustin M, Groves J. T-cell triggering thresholds are modulated by the number of antigen within individual T-cell receptor clusters. *Proc National Acad Sci.* 2011;108(22):9089–94. doi:10.1073/pnas.1018771108.
- Dreier T, Lorenczewski G, Brandl C, Hoffmann P, Srying U, Hanakam F, Kufer P, Riethmuller G, Bargou R, Baeuerle P. Extremely potent, rapid and costimulation-independent cytotoxic T-cell response against lymphoma cells catalyzed by a single-chain bispecific antibody. *Int J Cancer.* 2002;100(6):690–97. doi:10.1002/ijc.10557.
- Ding Q, Chen J, Wei X, Sun W, Mai J, Yang Y, Xu Y. RAFTsomes containing epitope-MHC-II complexes mediated CD4+ T cell activation and antigen-specific immune responses. *Pharm Res.* 2013;30(1):60–69. doi:10.1007/s11095-012-0849-7.
- Lo Y, Edidin M, Powell J. Selective activation of antigen-experienced T cells by anti-CD3 constrained on nanoparticles. *J Immunol.* 2013;191(10):5107–14. doi:10.4049/jimmunol.1301433.
- Fahmy T, Bieler J, Edidin M, Schneck J. Increased TCR avidity after T cell activation: a mechanism for sensing low-density antigen. *Immunity.* 2001;14(2):135–43. PMID: 11239446.
- Compte M, Álvarez-Cienfuegos A, Nuñez-Prado N, Sainz-Pastor N, Blanco-Toribio A, Pescador N, Sanz L, Alvarez-Vallina L. Functional comparison of single-chain and two-chain anti-CD3-based bispecific antibodies in gene immunotherapy applications. *OncoImmunology.* 2014;3(5):e28810. doi:10.4161/onci.28810.
- Kreutzman A, Ilander M, Porkka K, Vakkila J, Mustjoki S. Dasatinib promotes Th1-type responses in granzyme B expressing T-cells. *Oncoimmunology.* 2014;3:e28925. PMID: 25083322. doi:10.4161/onci.28925.
- Hanif A, Wang E, Thompson J, Baron J, Walsh M, Griffiths E. Combining blinatumomab with targeted therapy for BCR-ABL mutant relapsed/refractory acute lymphoblastic leukemia. *Leuk Lymphoma.* 2018;59(8):2011–13. doi:10.1080/10428194.2017.1411595.
- Mustjoki S, Petteri A, Dybedal I, Epling-Burnette P, Guilhot F, Hjorth-Hansen H, Höglund M, Kovanen P, Laurinolli T, Liesveld J, et al. Clonal expansion of T/NK-cells during tyrosine kinase inhibitor dasatinib therapy. *Blood.* 2008;23(8):1398–405. PMID: 19295545. doi:10.1038/leu.2009.46.

29. Yang Y, Liu C, Peng W, Lizée G, Overwijk W, Liu Y, Woodman S, Hwu P. Antitumor T-cell responses contribute to the effects of dasatinib on c-KIT mutant murine mastocytoma and are potentiated by anti-OX40. *Blood*. 2012;120(23):4533–43. doi:10.1182/blood-2012-02-407163.
30. Kreuzman A, Ladell K, Koechel C, Gostick E, Eklblom M, Stenke L, Melo T, Einsele H, Porkka K, Price D, et al. Expansion of highly differentiated CD8+ T-cells or NK-cells in patients treated with dasatinib is associated with cytomegalovirus reactivation. *Leukemia*. 2011;25(10):1587–97. PMID: 21647156. doi:10.1038/leu.2011.135.
31. Duré M, Macian F. IL-2 signaling prevents T cell anergy by inhibiting the expression of anergy-inducing genes. *Mol Immunol*. 2009;46(5):999–1006. doi:10.1016/j.molimm.2008.09.029.
32. Lechler R, Chai J, Marelli-Berg F, Lombardi G. The contributions of T-cell anergy to peripheral T-cell tolerance. *Immunology*. 2001;103(3):262–69. doi:10.1046/j.1365-2567.2001.01250.x.
33. Vafa O, Trinklein N. Perspective: designing T-cell engagers with better therapeutic windows. *Front Oncol*. 2020;10:446. PMID: 32351885. doi:10.3389/fonc.2020.00446.
34. Garcia-Lora A, Algarra I, Garrido F. MHC class I antigens, immune surveillance, and tumor immune escape. *J Cell Physiol*. 2003;195(3):346–55. doi:10.1002/jcp.10290.
35. Li H, Di J, Peng B, Xu Y, Zhang N. Surface ligand valency and immunoliposome binding: when more is not always better. *Pharm Res*. 2021;38(9):1593–600. doi:10.1007/s11095-021-03092-y.
36. Kim C, Axup J, Lawson B, Yun H, Tardif V, Choi S, Zhou Q, Dubrovskaya A, Biroc S, Marsden R, et al. Bispecific small molecule-antibody conjugate targeting prostate cancer. *Proc Natl Acad Sci USA*. 2013;110(44):17796–801. PMID: 24127589. doi:10.1073/pnas.1316026110.